



Transcriptomic context of *DRD1* is associated with prefrontal activity and behavior during working memory

Leonardo Fazio^{a,b,1}, Giulio Pergola^{a,1}, Marco Papalino^a, Pasquale Di Carlo^a, Anna Monda^a, Barbara Gelao^a, Nicola Amoroso^{c,d}, Sabina Tangaro^d, Antonio Rampino^{a,e}, Teresa Popolizio^b, Alessandro Bertolino^{a,e}, and Giuseppe Blasi^{a,e,2}

^aDepartment of Basic Medical Science, Neuroscience, and Sense Organs, University of Bari Aldo Moro, 70124 Bari, Italy; ^bSezione di Neuroradiologia, Istituto di Ricovero e Cura a Carattere Scientifico "Casa Sollievo della Sofferenza," 71013 San Giovanni Rotondo, Italy; ^cDipartimento Interateneo di Fisica "M. Merlin," Università degli Studi di Bari Aldo Moro, 70125 Bari, Italy; ^dSezione di Bari, Istituto Nazionale di Fisica Nucleare, 70125 Bari, Italy; and ^eInstitute of Psychiatry, Bari University Hospital, 70124 Bari, Italy

Edited by Solomon H. Snyder, Johns Hopkins University School of Medicine, Baltimore, MD, and approved April 10, 2018 (received for review October 12, 2017)

Dopamine D₁ receptor (D₁R) signaling shapes prefrontal cortex (PFC) activity during working memory (WM). Previous reports found higher WM performance associated with alleles linked to greater expression of the gene coding for D₁Rs (*DRD1*). However, there is no evidence on the relationship between genetic modulation of *DRD1* expression in PFC and patterns of prefrontal activity during WM. Furthermore, previous studies have not considered that D₁Rs are part of a coregulated molecular environment, which may contribute to D₁R-related prefrontal WM processing. Thus, we hypothesized a reciprocal link between a coregulated (i.e., coexpressed) molecular network including *DRD1* and PFC activity. To explore this relationship, we used three independent postmortem prefrontal mRNA datasets (total *n* = 404) to characterize a coexpression network including *DRD1*. Then, we indexed network coexpression using a measure (polygenic coexpression index—*DRD1*-PCI) combining the effect of single nucleotide polymorphisms (SNPs) on coexpression. Finally, we associated the *DRD1*-PCI with WM performance and related brain activity in independent samples of healthy participants (total *n* = 371). We identified and replicated a coexpression network including *DRD1*, whose coexpression was correlated with *DRD1*-PCI. We also found that *DRD1*-PCI was associated with lower PFC activity and higher WM performance. Behavioral and imaging results were replicated in independent samples. These findings suggest that genetically predicted expression of *DRD1* and of its coexpression partners stratifies healthy individuals in terms of WM performance and related prefrontal activity. They also highlight genes and SNPs potentially relevant to pharmacological trials aimed to test cognitive enhancers modulating *DRD1* signaling.

gene coexpression network | *DRD1* | working memory | fMRI | polygenic score

Decades of exploration of the relationship between dopamine (DA) and cognition have established a crucial role of prefrontal D₁ receptors (D₁Rs) in working memory (WM) (1–8). D₁Rs modulate prefrontal synaptic neurotransmission by mediating recurrent excitation in local circuits, which is considered a key WM mechanism (3, 9, 10). Furthermore, increased D₁R signaling enhances the signal-to-noise ratio in prefrontal neuronal networks (5) and contributes to improved WM performance in nonhuman primates (11). Further evidence also suggests that extreme hypo- or hyperstimulation of D₁Rs is detrimental to prefrontal physiology related to WM and predicts poorer WM performance (1, 6, 12, 13). Taken together, these results suggest that the level of D₁R signaling in the prefrontal cortex (PFC) is important for efficient WM processing. In particular, functional imaging studies in humans have considered lower prefrontal activity paralleled by higher or unaffected WM performance as a correlate of efficient WM processing (14).

Notably, WM behavior and related prefrontal activity have an estimated heritability around 0.4 (15–17), and the heritable

component of WM is associated with DA-related genetic variation (18). Given the primary role of D₁R signaling in WM, it has been hypothesized that, across individuals, differences in WM behavior and brain activity may be related to the genetics of D₁R signaling. Consistently, functional single nucleotide polymorphisms (SNPs) of the gene coding for D₁Rs (*DRD1*, located in the 5q35.2 region in chromosome 5) have been associated with cognition and executive function. For example, previous studies have reported that the A allele of *DRD1* rs686 predicts greater in vitro *DRD1* expression (18–20). Another *DRD1* SNP, rs5326, has been associated with gene expression in the temporal gyrus and with *DRD1* transcriptional activity in human neuroblastoma cells (19, 21). Additionally, the A allele, associated with lower *DRD1* expression, predicted poorer executive function estimates. Overall, this evidence suggests that *DRD1* functional genetic variants may explain part of the interindividual variability in WM performance. These findings

Significance

Dopamine D₁ receptors in the prefrontal cortex (PFC) are critical for working memory (WM). However, it is unknown how D₁-related genetic background mediates differences in WM performance between humans. Furthermore, previous studies did not consider that *DRD1* is likely part of a coregulated molecular network, which may contribute to WM performance and its underlying neural correlates. The key of this research is the identification of a relationship between genetically predicted coexpression and WM processing. In particular, genetically predicted greater *DRD1*-related coexpression was associated with lower PFC activity and higher WM performance, indicating greater WM efficiency. Our findings may help to link gene expression with brain activity and to develop WM-enhancing drugs by differentiating individuals based on their genetic background.

Author contributions: L.F., G.P., and G.B. designed the research; G.P., S.T., and A.B. provided access to data and research funding; L.F., B.G., and T.P. collected data; L.F., G.P., M.P., P.D.C., A.M., N.A., S.T., and A.R. analyzed the data; L.F., G.P., P.D.C., N.A., S.T., A.R., A.B., and G.B. interpreted the data; L.F. and G.P. wrote the paper; and M.P., P.D.C., A.M., B.G., N.A., S.T., A.R., T.P., A.B., and G.B. revised and edited versions of the paper.

Conflict of interest statement: A.B. is a stockholder of Hoffmann–La Roche Ltd. and has also received lecture fees from Otsuka, Janssen, and Lundbeck and consultant fees from Biogen. A.R. has received travel fees from Lundbeck. G.P. has been the academic supervisor of a Roche collaboration grant (years 2015–2016) that funds his salary and the salary of A.R. All other authors have no biomedical financial interests and no potential conflicts of interest.

This article is a PNAS Direct Submission.

Published under the PNAS license.

¹L.F. and G.P. contributed equally to this work.

²To whom correspondence should be addressed. Email: giuseppe.blasi@uniba.it.

This article contains supporting information online at www.pnas.org/lookup/suppl/doi:10.1073/pnas.1717135115/-DCSupplemental.

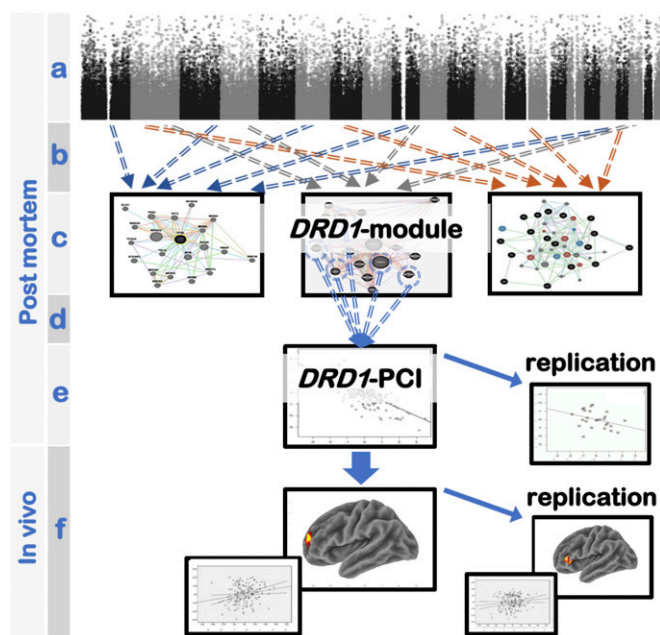


Fig. 1. Concept illustration of the study design. (A) Genome-wide genotyping; (B) Weighted Gene Coexpression Network Analysis identified modules of coexpressed genes; (C) prioritization of the coexpression module including *DRD1* (*DRD1*-module); (D) selection of the genes most associated with *DRD1* expression within the *DRD1*-module (*DRD1* gene set); (E) computation of a *DRD1* polygenic coexpression index, using genes within the *DRD1* gene set (*DRD1*-PCI); (F) association of *DRD1*-PCI with working memory performance and related brain activity.

also indicate that alleles associated with greater *DRD1* expression predict higher cognitive performance. However, previous works have fallen short of relating predicted gene expression of *DRD1* in the PFC with WM because the association between genetic variation and *DRD1* expression has not been studied in the human PFC. Furthermore, there is no evidence about the relationship between genetically determined *DRD1* expression and PFC activity during WM in humans.

Notably, *DRD1* has never been studied in the context of gene networks. Genes are expressed in coregulated networks (20), but little is currently known on (i) the interplay between *DRD1* and other genes in terms of gene expression regulation and (ii) the link between coregulated networks of genes including *DRD1* and prefrontal activity during WM. Therefore, the investigation of gene coexpression networks may yield more information and predictive power compared with those obtained by focusing on *DRD1* per se (20, 21). Additionally, recent studies have shown that combining multiple SNPs affords greater power on gene expression prediction studies compared with single SNP studies (22, 23).

On this basis, our aim was to identify a coexpression gene set including *DRD1* in the PFC and the genetic variants associated with the coexpression of the *DRD1*-related gene set. Furthermore, we investigated how genetically predicted coexpression of the *DRD1* gene set is associated with prefrontal WM processing. To this purpose, we refined an approach we have reported in a previous proof-of-concept work (21) (Fig. 1). Briefly, in the present work, after identifying a transcriptome-wide coexpression network in post-mortem human dorsolateral PFC (DLPFC) (Brodmann area 46), we selected the coexpression gene set including *DRD1*. Then, we identified SNPs associated with coexpression [coexpression quantitative trait loci (coeQTLs)] of such a gene set. Thus, we combined the effect of these SNPs on coexpression into an index (polygenic coexpression index—*DRD1*-PCI) predicting the coexpression of the *DRD1*-related gene set. Finally, we tested whether the *DRD1*-PCI was linked with interindividual variation in PFC activity and behavior during WM in two independent samples of healthy individuals

who participated in an N-back fMRI study. Based on previous studies (14, 18, 19), we expected that alleles predicting coexpression of the *DRD1* network and greater *DRD1* expression would also be associated with higher WM performance and lower PFC activity estimates, i.e., greater PFC efficiency. To account for potential effects of *DRD2* on the target phenotypes, we included our previously published *DRD2*-PCI in the fMRI and behavioral analyses.

Results

Weighted Gene Coexpression Network Analysis and Parceling. We used a previously reported gene coexpression network (21), based on the public dataset BrainCloud (24) (Tables 1 and 2) of transcriptome-wide dorsolateral PFC gene expression. Using a newly developed technique (25), we parceled the very large Weighted Gene Coexpression Network Analysis (WGCNA) module that included *DRD1* (2,452 genes) to identify a more focused coexpression gene set related with *DRD1* expression. The parceling procedure detailed the *DRD1* transcriptomic context, and we obtained a smaller coexpression set of 126 genes (*SI Appendix, Table S1*). We replicated the gene set structure using the BrainEAC dataset (26) and the RNA sequencing dataset published by the CommonMind Consortium (CMC) (27) (Tables 1 and 2) and found that these genes were more strongly connected than chance (BrainEAC $P = 0.0037$; CMC $P < 0.0001$) (*SI Appendix, Fig. S1C*). Additionally, we found that, in BrainEAC, 85 of 126 genes contributed to the first principal component of gene expression (module eigengene) in the same direction observed in BrainCloud, a higher-than-chance proportion (binomial test, $P = 5.7 \times 10^{-6}$). In CMC, 76 of 106 genes covaried just as observed in BrainCloud (binomial test, $P = 1.6 \times 10^{-6}$). Therefore, both gene connectivity and the direction of gene coexpression was largely preserved in two independent datasets. Neither the large module nor the restricted gene set included the *DRD2* gene, and we found no significant correlation between *DRD1* and *DRD2* ($n = 199$, Spearman's $\rho = 0.12$, $P = 0.09$). None of the genes in the *DRD1* set were in the *DRD2* module we previously published (21).

We investigated the biological functions of this gene set and found that protein binding genes (88 hits, 1.38-fold enrichment, Bonferroni corrected $P = 0.021$) and genes functionally associated with DNA-dependent ATPase activity (6 hits, 12-fold enrichment, Bonferroni corrected $P = 0.036$) were overrepresented. The first principal component of gene set expression (gene set eigengene, GSE), which we used as a coexpression measure, explained 50% of the gene set expression variance. *DRD1* belonged to a minority of 47 genes negatively correlated with the GSE (*SI Appendix, Fig. S1B*) ($R^2 = 0.38$, $P < 2.2 \times 10^{-16}$), suggesting that *DRD1* expression was higher when the expression of the majority of its partner genes was lower.

DRD1 Polygenic Coexpression Index Computation in Postmortem Tissue.

We first assessed whether SNPs in the genomic proximity of *DRD1* were associated with *DRD1* expression but found no significant hit (uncorrected $\alpha = 0.05$). Then, we identified SNPs associated with the GSE using previously reported methods (21). Out of 3,079 SNPs included in the coexpressed genes and their 100-kbp flanks, we obtained a set of 13 independent significant hits (Table 3 and *SI Appendix, Table S3*). The ensemble of the 13 SNPs selected and the genetic variants in full linkage disequilibrium with them ($R^2 = 1$) included more genetic regulatory elements than expected by chance in the DLPFC ($P = 0.03$) (28). We used these 13 SNPs to compute a

Table 1. Gene expression datasets used in the study

Datasets	Age	RIN	PMI	pH
BC (N199; 139♂; AA105)	32[20]	8.4[0.5]	30[15]	6.5[0.3]
BrainEAC (N26; 20♂; AA0)	62[17]	6.6[0.5]	43[28]	6.3[0.2]
CMC (N179; 115♂; AA34)	58[17]	8.1[0.6]	16[7]	6.6[0.3]

SDs are indicated between square brackets. AA, African American; BC, BrainCloud dataset; CMC, CommonMind Consortium dataset; N, sample size; PMI, postmortem interval in hours; RIN, RNA integrity number.

Table 2. fMRI and behavioral datasets used in the study

Datasets	Age	EHI	SES	IQ
f/b-DISC (N152; 78 δ)	27[7]	0.75[0.4]	43[16]	108[12]
f-REP (N149; 76 δ)*	28[7]	0.74[0.4]	41[17]	106[13]
b-REP (N193; 89 δ)*	27[8]	0.74[0.4]	39[17]	106[12]

SDs are indicated between square brackets. b-REP, behavioral replication sample; EHI, Edinburgh Handedness Inventory; f/b-DISC, fMRI and behavioral discovery sample; f-REP, fMRI replication sample; IQ, intelligence quotient; SES, socioeconomic status.

*f-REP and b-REP are partially overlapping (123 individuals in common).

polygenic coexpression index (PCI) associated with *DRD1* gene set coexpression (*DRD1*-PCI) (*SI Appendix*, Table S2 reports the weights attributed to all genotypes of these 13 SNPs). Additionally, we performed leave-one-out cross-validation on the SNP selection to estimate the reliability of the *DRD1*-PCI as a proxy of gene coexpression. We found that the *DRD1*-PCI significantly predicted the GSE in subjects not included in the training set ($R^2 = 0.024$, $P = 0.029$) (*SI Appendix*, Fig. S2). Since *DRD1* was negatively correlated with the GSE, we reversed the *DRD1*-PCI to have it positively correlated with *DRD1* expression for the sake of simplicity of graphic representation (*SI Appendix*, Fig. S2). We also screened possible associations of the *DRD1*-PCI with confounding variables [age, sex, ethnicity, RNA integrity number (RIN), pH, postmortem interval] and found a significantly higher *DRD1*-PCI in Caucasians than in African Americans (independent t test, $|t_{198}| = 2.9$, $P = 0.004$), likely because of the population stratification of allelic frequencies. Analysis of covariance (ANCOVA) on the cross-validated *DRD1*-PCI revealed no significant main effect of ethnicity on the GSE ($F_{1,195} = 0.44$; $P = 0.51$). Instead, the main effect of the leave-one-out cross-validated *DRD1*-PCI remained significant ($F_{1,195} = 5.23$; $P = 0.023$). There was no significant *DRD1*-PCI \times ethnicity interaction on GSE ($F_{1,195} = 0.08$; $P = 0.77$), suggesting no significant difference in the slope of the association across ethnicities. Indeed, the cross-validated *DRD1*-PCI was associated with the GSE both in African Americans and Caucasians with comparable effect sizes (Caucasians: $R^2 = 0.03$; African Americans: $R^2 = 0.022$) (*SI Appendix*, Fig. S3). The *DRD1*-PCI association with the GSE was replicated in the same direction in BrainEAC ($R^2 = 0.12$, one-tailed $P = 0.041$) (*SI Appendix*, Fig. S2) and in CMC ($R^2 = 0.017$, one-tailed $P = 0.043$) (*SI Appendix*, Fig. S2). Notably, the association was significant despite the differences between datasets (including ethnic differences) (Tables 1 and 2) and preprocessing procedures.

Association Between the *DRD1*-PCI and WM Processing. We tested the association between the *DRD1*-PCI and WM processing (29) in a sample of 371 unrelated healthy adult Caucasian volunteers (Tables 1 and 2).

fMRI. A general linear model was used to investigate the association between *DRD1*-PCI and brain activity using both linear and quadratic terms of the *DRD1*-PCI. The quadratic term of the *DRD1*-PCI was included to assess the documented U-shaped dose-response function between *DRD1* stimulation and PFC activity (5). We also included as a covariate the linear and quadratic term of the *DRD2*-PCI (21, 30), to control for potentially confounding effects. We found a negative association of the linear term of the *DRD1*-PCI with blood oxygen level-dependent (BOLD) response in the left PFC [middle frontal gyrus—Brodmann Area 10: $x, y, z = -29, 53, 24$; $F = 22.25$; $Z = 4.51$; family-wise error (FWE)-corrected cluster extent = 7 voxels, $\sim 345 \text{ mm}^3$, whole brain FWE-corrected $P = 0.006$] (Fig. 2 *A* and *C*). There were no other significant effects or interactions involving the *DRD1*-PCI. Similarly, in the fMRI replication sample, we found a negative association between the *DRD1*-PCI and activity in the left PFC, using the same whole brain statistical threshold (middle frontal gyrus—Brodmann Area 46: $x, y, z = -40, 34, 5$; $T = 4.41$; $Z = 4.26$; FWE-corrected cluster extent = 6 voxels, $\sim 316 \text{ mm}^3$, whole brain

FWE-corrected $P = 0.02$) (Fig. 2 *B* and *D*). These findings imply that the BOLD signal was lower in individuals with higher predicted *DRD1* expression, corresponding to lower predicted coexpression of the majority of the gene set.

Behavioral Results. We used differential WM accuracy [accuracy at the greater WM load minus accuracy at the lower WM load (Δ_{WM})] as a WM performance measure, as suggested by previous work (31). As in the fMRI study, we tested the association between *DRD1*-PCI and WM performance using both linear and quadratic terms of the *DRD1*-PCI and of the *DRD2*-PCI. In the discovery sample, the general linear model revealed a main effect of the linear term of the *DRD1*-PCI ($F_{1,144} = 6.3$; $P = 0.014$; partial $\eta^2 = 0.041$) (Fig. 2*E*) (see the *SI Appendix* for other effects). The *DRD1*-PCI correlated positively with Δ_{WM} , indicating higher WM capacity with greater predicted *DRD1* expression. The association of the *DRD1*-PCI with Δ_{WM} was also significant in the same direction in the replication sample ($t_{186} = 1.91$; one-tailed $P = 0.029$; partial $\eta^2 = 0.019$) (Fig. 2*F*). Therefore, individuals with alleles associated with higher *DRD1* expression and lower coexpression of the gene set had lower BOLD activity and higher behavioral performance.

To investigate the potential relationship between *DRD1*-related physiology, prefrontal activity, and other components of the dopaminergic system, such as *DRD2*, we used mediation and moderation analyses. Briefly, the analyses revealed significant mediation of prefrontal BOLD in the relationship between the *DRD1*-PCI and Δ_{WM} , and such mediation was moderated by the *DRD2*-PCI. However, the effects detected in the discovery sample failed to replicate and are reported in *SI Appendix*, *Mediation Analysis*.

Discussion

Multiple lines of evidence suggest that D_1R signaling exerts a key effect on WM performance and WM-related brain activity. It has been hypothesized that *DRD1* genetic variation may affect D_1R signaling, e.g., by affecting *DRD1* expression (18, 19). However, to our knowledge, there is no evidence of association of *DRD1* genetic variation with gene expression in the PFC. More importantly, there are no previous studies addressing how genetic ensembles related to *DRD1* affect prefrontal function during WM. The *DRD1*-PCI that we generated in the present study is an index of predicted coexpression of a *DRD1*-related gene set in the PFC. We found that this polygenic index was associated with WM behavior and related PFC activity across independent samples. In particular, the greater the *DRD1*-PCI, the higher the differential accuracy and the lower the PFC response during the N-back. These relationships survived, even considering the effect of

Table 3. Ranked single nucleotide polymorphisms (SNPs) included in the computation of the *DRD1*-PCI

SNP (module gene)	Association with		
	GSE	CG	<i>DRD1</i>
rs7487813 (<i>UBE2M</i>)	2.22×10^{-5}	0.003	0.009
rs2267844 (<i>SLC26A6</i>)	1.43×10^{-4}	0.013	0.007
rs663208 (<i>CCDC81</i>)	3.71×10^{-4}	0.013	0.031
rs17005918 (<i>SCOC</i>)	4.51×10^{-4}	0.001	0.002
rs13101217 (<i>SEC22A</i>)	5.35×10^{-4}	0.015	0.006
rs1859464 (<i>PCNX1</i>)	9.22×10^{-4}	0.707	0.002
rs2278214 (<i>MGAT4A</i>)	1.21×10^{-3}	0.009	0.001
rs7915524 (<i>FAM171A1</i>)	2.05×10^{-3}	0.207	0.256
rs12509826 (<i>SCOC</i>)	3.67×10^{-3}	0.004	0.189
rs10134399 (<i>XRCC3</i>)	4.26×10^{-3}	0.079	0.095
rs10906841 (<i>FAM171A1</i>)	4.52×10^{-3}	0.003	0.356
rs2306251 (<i>GAK</i>)	4.61×10^{-3}	0.118	0.12
rs11602122 (<i>TPCN2</i>)	4.83×10^{-3}	0.221	0.005

The association columns report the P values of the association. The expression of genes reported in bold font is negatively correlated with the gene set eigengene, as is also the case of *DRD1*. CG, closest gene; GSE, gene set eigengene.

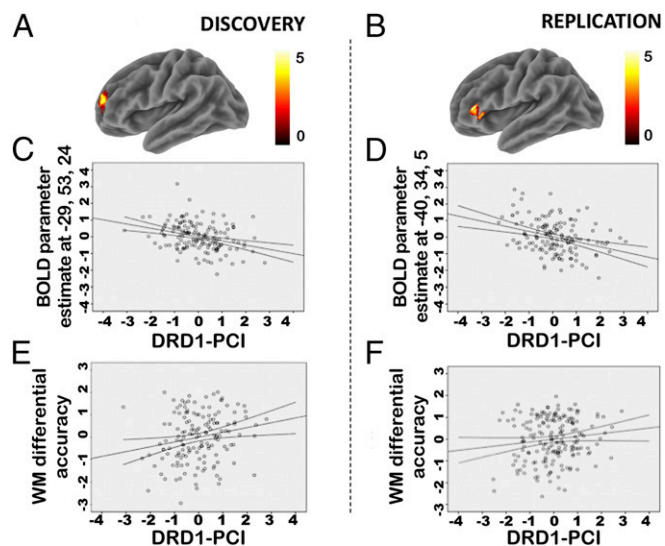


Fig. 2. Association of the *DRD1*-PCI with working memory-related prefrontal activity and working memory performance. (A) Rendering of the brain activity significantly associated in the discovery sample with *DRD1*-PCI in the dorsolateral prefrontal cortex, and color bar with the relative Z scores. (B) Rendering of the brain activity significantly associated in the replication sample with *DRD1*-PCI in the dorsolateral prefrontal cortex, and color bar with the relative Z scores. Left in the figures is left in the brain. (C and D) Scatter plots of the Z scores of the estimated activity in these clusters (y axis) as a function of the Z score of the *DRD1*-PCI. (C) Discovery sample; (D) replication sample. (E and F) Scatter plots show the Z score of the *DRD1*-PCI on the x axis and differential accuracy on the y axis. (E) Discovery sample; here the y axis reports the average of the two loads (Δ_{2-1} and Δ_{3-2}) after marginalization for covariates and standardization. (F) Replication sample; here, the y axis reports Δ_{2-1} after marginalization for covariates and standardization. Plots show trend lines and 95% confidence intervals of the mean.

another component of the dopaminergic system, *DRD2*, indexed by the *DRD2*-PCI. Based on previous models positing that greater PFC activity despite similar or lower behavioral proficiency is a correlate of less efficient WM processing (4, 7, 14), these results suggest that greater predicted *DRD1* expression and lower coexpression of the *DRD1*-related gene set are associated with greater WM efficiency.

The Genetic Architecture of *DRD1* Transcription. The gene set we identified is reproducibly coexpressed, as shown by the replication in two independent datasets (26); further, this gene set seems independent of the transcriptomic context of *DRD2*. It is noteworthy that the majority of the genes in this set are down-regulated when *DRD1* is up-regulated. Gene ontology analysis revealed that genes related with DNA helicase activity were overrepresented in this set. Additionally, two of the SNPs that we identified as coeQTLs (rs7487813 and rs10134399) map close to genes in the coexpression gene set that are associated with DNA double-strand break repair (*UBE2N* and *XRCC3*). Both SNPs are associated, albeit weakly, with the expression of the respective genes (Table 3) (rs10134399 is associated with *XRCC3* in an independent study) (32). Double-strand DNA breaks have been highlighted as a mechanism linking neuronal activity with transcription regulation (33). Based on this activity–transcription relationship, the fact that *DRD1* expression covaries with that of genes related with double-strand DNA break repair may suggest a link between *D1R*-related neuronal activity and transcription mechanisms of the *DRD1*-related gene set. Even if this contention is speculative based on the current results, relationships between transcription levels and brain activity are supported by the literature (34). The evidence we report may be used to select partner genes of *DRD1* as candidate genes for mechanistic investigations of the link between *D1R* activity and *DRD1* gene set transcription levels in cell biology experiments.

The Role of Prefrontal *D1* Receptors in Working Memory. *D1R* signaling supports WM-related persistent neural firing in the PFC (3, 10), allowing greater focus of neural resources on the task at hand (5). According to the model put forward by Seamans and Yang (5), *D1R*s enhance the signal-to-noise ratio in PFC neurons during WM performance by promoting activity in recurrent circuits. *D1R*s are thought to act via a specific block of task-unrelated excitatory inputs in the PFC (6, 10, 35). Consistently, small increases in *D1R* signaling have been linearly correlated with WM behavior (10, 11, 36–38). Furthermore, previous findings indicated poorer WM performance in genetic or clinical conditions associated with reduced *DRD1* expression (19, 39, 40). Overall, the present results are consistent with these previous findings. In fact, greater predicted *DRD1* expression—as inferred based on its coexpression gene set—was associated with lower PFC activity, which has been consistently interpreted as a correlate of greater prefrontal efficiency during WM (14). Furthermore, greater predicted *DRD1* expression was also associated with higher WM behavioral accuracy. These findings also suggest that the regulation of *DRD1* expression is polygenic, rather than only based on genetic variants proximal to *DRD1*, and is embedded in the context of gene network coexpression.

Seamans and Yang (5) posited that excessive levels of *D1R*s impair WM performance (inverted-U model of WM function). Both animal (35) and human studies (41) support this interpretation. However, we found that the quadratic component of the PCI did not provide a significant fit either in brain or in behavioral phenotypes. It should be noted that we evaluated a genetic component associated with physiological variation in *DRD1* transcription levels in healthy individuals. Thus, a possible interpretation of our results is that we investigated variation within the physiological portion of the inverted-U curve—pharmacological stimulation or more extreme genotypic configurations may be necessary to observe the full inverted-U curve.

Limitations. The SNP set we used to compute the *DRD1*-PCI does not include variants that are significantly associated with coexpression per se because we used an uncorrected statistical threshold. Instead, we identified a set of 13 SNPs which, together, explain part of the coexpression of the *DRD1* gene set. Consistent with a putative role of the SNPs here identified as functional variants, previously reported regulatory variants of gene expression in the DLPFC were overrepresented in this SNP set. Further issues to be addressed are the different localization of the clusters identified in the discovery and replication samples and the lack of replication of the mediation and moderation analyses. Both the discovery and replication clusters were located in PFC regions relevant for WM (2). While relaxing the threshold revealed a substantial overlap between the clusters ($P < 0.05$, $x, y, z = -40, 12, 9$; $Z = 2.28$; $k = 37$), sample characteristics and study protocols may explain the difference in spatial localization when more stringent statistical thresholds are used. It remains noteworthy that the effect of the *DRD1*-PCI was significant in the PFC in the same direction in two independent samples, despite the different protocols employed.

Conclusions

The present results shed light on the understanding of the genetic modulation of WM-related phenotypes via *D1R*s and their transcriptomic context. Since the functional variants in multiple genes coexpressed with *DRD1* allow in vivo prediction of *DRD1* expression in the DLPFC, they may be relevant to clinical conditions associated with dysregulation of this gene (40). For example, clinical trials using *D1R* agonists on patients with schizophrenia failed to demonstrate amelioration of cognitive symptoms (42). Thus, our findings may help in developing WM-enhancing drugs for clinical populations, acting on *D1R*s (42, 43), in a personalized medicine framework. Such an approach could be especially relevant for clinical conditions characterized by pervasive WM deficits like dementia, schizophrenia, and bipolar disorder (44–46).

Materials and Methods

Gene Coexpression Network Analysis in Postmortem PFC. We used Braincloud (24) (Tables 1 and 2) and Weighted Gene Coexpression Network Analysis (WGCNA) to obtain a transcriptome-wide coexpression network in the post-mortem DLPFC of 199 individuals free of psychiatric and neurologic diseases. We used the same transcriptome-wide coexpression network published in our previous work (21), with the same subjects, without identifying a new network. Briefly, in our previous work, we selected postnatal samples from Caucasian and African American subjects with RNA integrity (RIN) >7.0, to ensure high data quality (47), and preprocessed the data to reduce the effect of confounders [demographical variables (i.e., age, sex, ethnicity) and sample quality features (i.e., RIN, pH, postmortem interval); see the *SI Appendix* for details]. *DRD1* clustered within a module including 2,452 probes. In this module, *DRD1* was not a hub gene (scaled within-module connectivity was close to the median). The module did not include any probes of the gene *DRD2*. The number of probes in this module was very high and difficult to study as a single unit. Recent evidence shows that further parceling of WGCNA modules can improve the detection of robust gene sets (48). To obtain the parceling, we used the hard-thresholding procedure described by Monaco et al. (49) based on the topological properties of the module (50, 51) (*SI Appendix*). Throughout the manuscript, we refer to this subset of coexpressed genes within the WGCNA *DRD1* module as the “*DRD1* gene set.” Then, we investigated the biological functions of this gene set by using the software AMIGO2 (amigo2.geneontology.org/amigo) to assess the overrepresentation of gene ontology labels. Next, we sought to replicate in independent datasets the connectivity between members of the *DRD1* parceled gene set. With this aim, we used the publicly available dataset BrainEAC (www.braineac.org/) and the CommonMind Consortium (CMC) RNA sequencing data derived from post-mortem human PFC (27) (Tables 1 and 2 and *SI Appendix*). We preprocessed BrainEAC and CMC expression values using the remove unwanted variation algorithm (RUV) designed to identify and subsequently remove latent confounding factors (52) (*SI Appendix*). We did not use explicit confounders. In Braincloud, we kept the original WGCNA for consistency with our prior work. Then, we used the permutation procedure described by Johnson et al. (53) (10,000 permutations) to test whether the gene–gene relationships between *DRD1* coexpression partners was significantly greater than a null distribution of random gene expression in these independent datasets. Finally, we asked whether gene expression covariation in both replication datasets had the same direction observed in Braincloud (*SI Appendix*).

***DRD1* Polygenic Coexpression Index Computation.** To assess whether gene-specific eQTLs predicted *DRD1* expression, we performed a local eQTL study by associating SNPs within 100 kbp up- and downstream *DRD1* with *DRD1* expression, as done in previous work (23). Then, we associated the GSE with SNPs to identify a pool of SNPs that, together, reliably predict coexpression. Hence, our aim was not to identify SNPs that, on their own right, predict coexpression—which requires statistics corrected for multiple comparisons. We selected SNPs falling into a window of 100 kbp up- and downstream the start and end position of each gene in the *DRD1* gene set (as in previous works) (21, 23) (see the *SI Appendix* for further selection criteria). To select SNPs included in the *DRD1*-PCI, we used the same criterion published by Pergola et al. (21): i.e., uncorrected $P < 0.005$ in the association with the GSE (*SI Appendix*). We also assessed the biological significance of the SNP set identified by interrogating the software Haploreg v. 4.1 (archive.broadinstitute.org/mammals/haploreg/haploreg.php) (28). Using Haploreg, we computed the statistics for overrepresentation of DLPFC (BA9/46) regulatory elements in our list of SNPs; note that also Braincloud data were obtained from BA46. Further analyses investigated the association of these SNPs with *DRD1* and other module genes (*SI Appendix*). Once we identified the SNPs associated with coexpression of the *DRD1*-related gene set, we generated the *DRD1*-PCI predicting the combined effect of such SNPs on *DRD1* GSE. This index actually refers to the entire gene set, and not just to *DRD1*; we indicate it by this name because we selected a priori the module including *DRD1* to investigate the transcriptomic context of this gene, which is key to WM performance and its underlying brain activity. The index computation is based on the signal detection theory and quantifies the magnitude of the differences between genotypic populations of each of the SNPs selected (*SI Appendix*). After validating the *DRD1*-PCI by means of cross-validation (*SI Appendix*), we replicated the association of the *DRD1*-PCI with the GSE using BrainEAC/CMC frontal cortex total gene expression data and genotypes. For these replications, we replaced genotypes with the weights detected in Braincloud. Based on the results in the Braincloud sample, we tested the negative correlations between the *DRD1*-PCI and replication GSEs using one-tailed P values (we were only interested in associations with the same direction in both the discovery and replication samples).

Assessment of WM Processing in Healthy Humans.

Participants. Three hundred and seventy-one unrelated adult Caucasian individuals participated in the study (Tables 1 and 2) (106 of them were also included in our recently published work on the *DRD2*-PCI) (21) and were genome-wide genotyped using previously published procedures (54). One hundred and fifty-two subjects formed the discovery sample for the fMRI and the behavioral study and performed the 1-, 2-, and 3-Back runs of the N-Back WM task (29). Furthermore, separate cohorts of 149 and 193 participants formed, respectively, the replication sample for the fMRI study (only 2-Back acquired) and the behavioral study (only 1- and 2-Back acquired). Inclusion criteria and sociodemographic assessments are detailed in *SI Appendix*. The present study was approved by the local IRB at the University of Bari Aldo Moro. Written informed consent was obtained from all participants after full explanation of all procedures, which were carried out according to the Declaration of Helsinki.

Neuropsychological task. We used the widely adopted N-back task to probe WM (14) in both the behavioral and the fMRI studies (*SI Appendix*). During fMRI, we used three runs of a block design version of the task: 1-Back vs. 0-Back; 2-Back vs. 0-Back, and 3-Back vs. 0-Back (named 01-Back, 02-Back, and 03-Back, respectively), each lasting 240 s. Participants in the fMRI replication sample performed the 02-Back run only. Participants included in the behavioral discovery sample performed three blocks of all of the three WM conditions, while those included in the behavioral replication sample performed 1-Back and 2-Back.

Imaging study. Blood oxygen level-dependent (BOLD) signal was recorded by a GE Signa 3T scanner (General Electric), using a gradient-echo planar imaging sequence to acquire 120 volumes for each N-Back run. We used Statistical Parametric Mapping 12 (SPM12) (www.fil.ion.ucl.ac.uk/spm) to analyze the fMRI data using standard procedures (55) (*SI Appendix*). Since we developed a continuous predictor of *DRD1* expression, we had the opportunity to control for nonlinear effects using the quadratic term of the *DRD1*-PCI as a covariate both in the behavioral and imaging analyses. In the fMRI discovery sample, we tested the association of the *DRD1*-PCI with brain activation using a general linear model (see the *SI Appendix* for model specification). We used F contrasts to investigate the association between *DRD1*-PCI and brain activity using both linear and quadratic terms of the *DRD1*-PCI. We masked results selecting the voxels in which the activity was higher during WM than the baseline to select areas belonging to the WM brain network. This brain network is the most plausible set of regions likely affected by the transcriptomic context of *DRD1* during this cognitive process. We generated the WM activity mask by identifying areas significantly activated separately per load (1-back versus 0-back, 2-back versus 0-back, and 3-back versus 0-back) and computed the conjunction null contrast between the three loads (whole-brain $P = 0.05$, uncorrected) (*SI Appendix*, Fig. S4). To correct the results of the linear and quadratic terms of the PCI for multiple comparisons, we used the stringent voxel-wise threshold of $P < 0.05$, whole-brain FWE-corrected, with a minimum extent of five voxels ($\sim 264 \text{ mm}^3$). To further detail our results, we displayed these clusters at $P < 0.001$, uncorrected, in the figures. We additionally explored the relationship between WM-related brain activity, WM performance, and *DRD1*-PCI, as well as the interaction with *DRD2*-PCI using mediation and moderation models (*SI Appendix*). In the replication sample, we computed an ANCOVA on the 2-Back > 0-Back contrast, using the same whole-brain FWE correction. Based on the results in the discovery sample, we computed only a t test on the negative linear term of the *DRD1*-PCI regression slope. Results are shown using the same criteria followed in the discovery sample and masked with the same WM network mask.

Behavioral analyses. We used differential WM accuracy [accuracy at the greater WM load minus accuracy at the lower WM load (Δ_{WM})] as a WM capacity measure (30, 31). This measure is associated with the increase of cognitive load in N-back sessions performed outside the scanner. It usually takes negative values and is a direct measure of WM capacity: i.e., greater values of differential accuracy indicate consistent WM performance in the face of load increase. In the behavioral discovery sample, we computed the differential accuracy between 2-Back and 1-Back (Δ_{2-1}) and between 3-Back and 2-Back (Δ_{3-2}) (31). Thus, we computed a repeated measures general linear model. For the behavioral replication sample, only Δ_{2-1} was available, and it was included in a general linear model (see the *SI Appendix* for model specification).

ACKNOWLEDGMENTS. Permission to use the CommonMind Consortium dataset was graciously provided to G.P. by the National Institute of Mental Health (NIMH). Brain tissue for the CMC study was obtained from the following brain bank collections: the Mount Sinai NIH Brain and Tissue Repository, the University of Pennsylvania Alzheimer’s Disease Core Center, the University of Pittsburgh NeuroBioBank and Brain and Tissue Repositories, and the NIMH Human Brain Collection Core. The CMC leadership is as follows: Pamela Sklar, Joseph Buxbaum (Icahn School of Medicine at Mount Sinai), Bernie Devlin, David Lewis (University of Pittsburgh), Raquel Gur, Chang-Gyu Hahn (University of Pennsylvania),

Keisuke Hirai, Hiroyoshi Toyoshiba (Takeda Pharmaceuticals Company Limited), Enrico Domenici, Laurent Essioux (F. Hoffman-La Roche Ltd.), Lara Mangravite, Mette Peters (Sage Bionetworks), Thomas Lehner, and Barbara Lipska (NIMH). Data acquisition was made possible by Dr. Linda A. Antonucci, Riccarda Lomuscio, Dr. Marina Mancini, Rita Masellis, Dr. Annamaria Porcelli, Tiziana Quarto, Dr. Raffaella Romano, and Dr. Paolo Taurisano (University of Bari Aldo Moro). We also gratefully acknowledge the work by Prof. Roberto Bellotti, Dr. Pierluigi Selvaggi, Dr. Alfonso Monaco, Nicola Manzari, Roberta Passiatore, Graziella Amico, and Nicoletta Trotta (University of Bari Aldo Moro), who contributed to data analysis. Finally, we thank all the volunteers who took part in the study. This work was supported by a "Capitale Umano ad Alta Qualificazione" grant by Fondazione Con Il Sud, by National Alliance for Research on Schizophrenia

and Depression Grant 28935, by "Ricerca Finalizzata" Grant PE-2011-02347951 (to A.B.), and by a Hoffmann-La Roche Collaboration Grant (to G.P.). This project received funding from the European Union Seventh Framework Programme for research, technological development, and demonstration under Grant Agreement 602450. Data were generated as part of the CommonMind Consortium supported by funding from Takeda Pharmaceuticals Company Limited, F. Hoffman-La Roche Ltd., and NIH Grants R01MH085542, R01MH093725, P50MH066392, P50MH080405, R01MH097276, R01-MH-075916, P50M096891, P50MH084053S1, R37MH057881 and R37MH057881S1, HHSN271201300031C, AG02219, AG05138, and MH06692. This paper reflects only the authors' views, and the European Union is not liable for any use that may be made of the information contained therein.

- Goldman-Rakic PS (1990) Cellular and circuit basis of working memory in prefrontal cortex of nonhuman primates. *Prog Brain Res* 85:325–335; discussion 335–336.
- Rottschy C, et al. (2012) Modelling neural correlates of working memory: A coordinate-based meta-analysis. *Neuroimage* 60:830–846.
- Fuster JM, Alexander GE (1971) Neuron activity related to short-term memory. *Science* 173:652–654.
- D'Esposito M, Postle BR (2015) The cognitive neuroscience of working memory. *Annu Rev Psychol* 66:115–142.
- Seamans JK, Yang CR (2004) The principal features and mechanisms of dopamine modulation in the prefrontal cortex. *Prog Neurobiol* 74:1–58.
- Jacob SN, Stalter M, Nieder A (2016) Cell-type-specific modulation of targets and distractors by dopamine D1 receptors in primate prefrontal cortex. *Nat Commun* 7:13218.
- Van Snellenberg JX, et al. (2015) Dynamic shifts in brain network activation during supracapacity working memory task performance. *Hum Brain Mapp* 36:1245–1264.
- Blokland GA, et al. (2008) Quantifying the heritability of task-related brain activation and performance during the N-back working memory task: A twin fMRI study. *Biol Psychol* 79:70–79.
- Gao WJ, Krimer LS, Goldman-Rakic PS (2001) Presynaptic regulation of recurrent excitation by D1 receptors in prefrontal circuits. *Proc Natl Acad Sci USA* 98:295–300.
- Arnsten AF, Jin LE (2014) Molecular influences on working memory circuits in dorsolateral prefrontal cortex. *Prog Mol Biol Transl Sci* 122:211–231.
- Vijayraghavan S, Wang M, Birnbaum SG, Williams GV, Arnsten AF (2007) Inverted-U dopamine D1 receptor actions on prefrontal neurons engaged in working memory. *Nat Neurosci* 10:376–384.
- Paspalas CD, Goldman-Rakic PS (2005) Presynaptic D1 dopamine receptors in primate prefrontal cortex: Target-specific expression in the glutamatergic synapse. *J Neurosci* 25:1260–1267.
- Williams GV, Castner SA (2006) Under the curve: Critical issues for elucidating D1 receptor function in working memory. *Neuroscience* 139:263–276.
- Callicott JH, et al. (1999) Physiological characteristics of capacity constraints in working memory as revealed by functional MRI. *Cereb Cortex* 9:20–26.
- Blokland GA, et al. (2011) Heritability of working memory brain activation. *J Neurosci* 31:10882–10890.
- Fletcher JM, Marks AD, Hine DW, Coventry WL (2014) Heritability of preferred thinking styles and a genetic link to working memory capacity. *Twin Res Hum Genet* 17:526–534.
- Hansell NK, et al. (2015) Genetic basis of a cognitive complexity metric. *PLoS One* 10: e0123886.
- Baetu I, Burns NR, Urry K, Barbante GG, Pitcher JB (2015) Commonly-occurring polymorphisms in the COMT, DRD1 and DRD2 genes influence different aspects of motor sequence learning in humans. *Neurobiol Learn Mem* 125:176–188.
- Tsang J, et al. (2015) The relationship between dopamine receptor D1 and cognitive performance. *NPJ Schizophr* 1:14002.
- Gaiteri C, Ding Y, French B, Tseng GC, Sibille E (2014) Beyond modules and hubs: The potential of gene coexpression networks for investigating molecular mechanisms of complex brain disorders. *Genes Brain Behav* 13:13–24.
- Pergola G, et al. (2017) DRD2 co-expression network and a related polygenic index predict imaging, behavioral and clinical phenotypes linked to schizophrenia. *Transl Psychiatry* 7:e1006.
- Gamazon ER, et al.; GTEx Consortium (2015) A gene-based association method for mapping traits using reference transcriptome data. *Nat Genet* 47:1091–1098.
- Pergola G, et al. (2016) Combined effect of genetic variants in the GlnN2B coding gene (GRIN2B) on prefrontal function during working memory performance. *Psychol Med* 46:1135–1150.
- Colantuoni C, et al. (2011) Temporal dynamics and genetic control of transcription in the human prefrontal cortex. *Nature* 478:519–523.
- Monda A, et al. (2017) Topological complex networks properties for gene community detection strategy: DRD2 case study. *Emergent Complexity from Nonlinearity, in Physics, Engineering and the Life Sciences: Proceedings of the XXIII International Conference on Nonlinear Dynamics of Electronic Systems*, eds Mantica G, Stoop R, Stramaglia S (Springer International Publishing AG, Cham, Switzerland), Vol 191, pp 199–208.
- Trabzuni D, et al. (2011) Quality control parameters on a large dataset of regionally dissected human control brains for whole genome expression studies. *J Neurochem* 119:275–282.
- Fromer M, et al. (2016) Gene expression elucidates functional impact of polygenic risk for schizophrenia. *Nat Neurosci* 19:1442–1453.
- Ward LD, Kellis M (2012) HaploReg: A resource for exploring chromatin states, conservation, and regulatory motif alterations within sets of genetically linked variants. *Nucleic Acids Res* 40:D930–D934.
- Callicott C (1999) A magnetic field control system for a variable field NMR spectrometer. *Phys Med Biol* 44:N193–N199.
- Selvaggi P, et al. (2018) Genetic variation of a DRD2 co-expression network is associated with changes in prefrontal function after D2 receptors stimulation. *Cereb Cortex*, 10.1093/cercor/bhy022.
- Cassidy CM, et al. (2016) Dynamic connectivity between brain networks supports working memory: Relationships to dopamine release and schizophrenia. *J Neurosci* 36:4377–4388.
- Jaffe AE, et al. (2017) Developmental and genetic regulation of the human cortex transcriptome in schizophrenia. bioRxiv:10.1101/124321.
- Cholewa-Waclaw J, et al. (2016) The role of epigenetic mechanisms in the regulation of gene expression in the nervous system. *J Neurosci* 36:11427–11434.
- Richiardi J, et al.; IMAGEN consortium (2015) BRAIN NETWORKS. Correlated gene expression supports synchronous activity in brain networks. *Science* 348:1241–1244.
- Avery MC, Krichmar JL (2015) Improper activation of D1 and D2 receptors leads to excess noise in prefrontal cortex. *Front Comput Neurosci* 9:31.
- Ott T, Jacob SN, Nieder A (2014) Dopamine receptors differentially enhance rule coding in primate prefrontal cortex neurons. *Neuron* 84:1317–1328.
- Zahrt J, Taylor JR, Mathew RG, Arnsten AF (1997) Supranormal stimulation of D1 dopamine receptors in the rodent prefrontal cortex impairs spatial working memory performance. *J Neurosci* 17:8528–8535.
- Müller U, von Cramon DY, Pollmann S (1998) D1- versus D2-receptor modulation of visuospatial working memory in humans. *J Neurosci* 18:2720–2728.
- Huang W, Li MD (2009) Differential allelic expression of dopamine D1 receptor gene (DRD1) is modulated by microRNA miR-504. *Biol Psychiatry* 65:702–705.
- Kaalund SS, et al. (2014) Contrasting changes in DRD1 and DRD2 splice variant expression in schizophrenia and affective disorders, and associations with SNPs in postmortem brain. *Mol Psychiatry* 19:1258–1266.
- Gibbs SE, D'Esposito M (2006) A functional magnetic resonance imaging study of the effects of pergolide, a dopamine receptor agonist, on component processes of working memory. *Neuroscience* 139:359–371.
- Girgis RR, et al. (2016) A proof-of-concept, randomized controlled trial of DAR-0100A, a dopamine-1 receptor agonist, for cognitive enhancement in schizophrenia. *J Psychopharmacol* 30:428–435.
- McClure MM, et al. (2010) Pergolide treatment of cognitive deficits associated with schizotypal personality disorder: Continued evidence of the importance of the dopamine system in the schizophrenia spectrum. *Neuropsychopharmacology* 35:1356–1362.
- Brandt CL, et al. (2014) Working memory networks and activation patterns in schizophrenia and bipolar disorder: Comparison with healthy controls. *Br J Psychiatry* 204:290–298.
- Forbes NF, Carrick LA, McIntosh AM, Lawrie SM (2009) Working memory in schizophrenia: A meta-analysis. *Psychol Med* 39:889–905.
- Kirova AM, Bays RB, Lagalwar S (2015) Working memory and executive function decline across normal aging, mild cognitive impairment, and Alzheimer's disease. *BioMed Res Int* 2015:748212.
- Schroeder A, et al. (2006) The RIN: An RNA integrity number for assigning integrity values to RNA measurements. *BMC Mol Biol* 7:3.
- Botia JA, et al.; United Kingdom Brain Expression Consortium (2017) An additional k-means clustering step improves the biological features of WGCNA gene co-expression networks. *BMC Syst Biol* 11:47.
- Monaco A, et al. (2018) A complex network approach reveals a pivotal substructure of genes linked to schizophrenia. *PLoS One* 13:e0190110.
- Barrat A, Barthélemy M, Pastor-Satorras R, Vespignani A (2004) The architecture of complex weighted networks. *Proc Natl Acad Sci USA* 101:3747–3752.
- Shannon CE (1948) A mathematical theory of communication. *Bell Syst Tech J* 27:379–423.
- Freytag S, Gagnon-Bartsch J, Speed TP, Bahlo M (2015) Systematic noise degrades gene co-expression signals but can be corrected. *BMC Bioinformatics* 16:309.
- Johnson MR, et al. (2016) Systems genetics identifies a convergent gene network for cognition and neurodevelopmental disease. *Nat Neurosci* 19:223–232.
- Rampino A, et al. (2017) Association of functional genetic variation in PP2A with prefrontal working memory processing. *Behav Brain Res* 316:125–130.
- Friston KJ, Williams S, Howard R, Frackowiak RS, Turner R (1996) Movement-related effects in fMRI time-series. *Magn Reson Med* 35:346–355.